Published in final edited form as:
J Immunol. 2017 September 01; 199(5): 1796–1804. doi:10.4049/jimmunol.1602069.

Modulation of Roquin function in myeloid cells reduces *Mycobacterium tuberculosis* induced inflammation

Gayathri Nagalingam[*], **Carola G. Vinuesa**[#], **Warwick J Britton**[*,¶], and **Bernadette M. Saunders**[*,§,1]

[*]Tuberculosis Research Program, Centenary Institute, Newtown, NSW, 2042, Australia

[¶]Disciplines of Medicine, Infectious Diseases and Immunology, Sydney Medical School, University of Sydney, Sydney, NSW, 2006, Australia

[#]Department of Immunology and Infectious Disease, John Curtin School of Medical Research, The Australian National University, Canberra, ACT 2601, Australia

[§]School of Life Sciences, Faculty of Science, University of Technology Sydney, Ultimo, 2007, Australia

Abstract

Damaging inflammation is a hallmark of *Mycobacterium tuberculosis* infection, and understanding how this is regulated is important for the development of new therapies to limit excessive inflammation. The E3 ubiquitin ligase, Roquin, is involved in immune regulation, however its role in immunity to *M. tuberculosis* is unknown. To address this we infected mice with a point mutation in *Roquin1/Rc3h1* (*sanroque*). Aerosol-infected *sanroque* mice showed enhanced control of *M. tuberculosis* infection associated with delayed bacterial dissemination and upregulated TNF production in the lung after 2 weeks. However, this early control of infection was not maintained, and by 8 weeks post-infection *sanroque* mice demonstrated increased bacterial burden and dysregulated inflammation in the lung. As the inflammation in the lung of the *sanroque* mice could have been influenced by emerging autoimmune conditions that are characteristic of aging *sanroque* mice, the function of Roquin was examined in immune cell subsets in the absence of autoimmune complications. *Mycobacterium bovis* BCG-primed *sanroque* T cells transferred into *Rag1*$^{-/-}$ mice provided equivalent protection in the spleen and liver. Interestingly, the transfer of mycobacteria-specific (P25 CD4^{+} TCR transgenic) wild-type spleen cells into *sanroque.Rag1*$^{-/-}$ mice actually led to enhanced protection with reduced bacterial load, decreased chemokine expression and reduced inflammation in the lung compared with transfers into *Rag1*$^{-/-}$ mice expressing intact Roquin. These studies suggest that modulation of Roquin in myeloid cells may reduce both inflammation and bacterial growth during the chronic phase of *M. tuberculosis* infection.

Keywords

Roquin; *M. tuberculosis*; *sanroque*; T follicular helper cells; TNF; macrophages

[1]Corresponding author: Dr BM Saunders, Bernadette.Saunders@uts.edu.au, Phone: +61 2 9514 8311.

Europe PMC Funders Author Manuscripts

Introduction

Tuberculosis (TB) is a chronic respiratory disease caused by *M. tuberculosis* and the leading cause of death from a single pathogen worldwide [1]. The host's immune response to the pathogen is a major determinant of outcome following *M. tuberculosis* infection. Protection against *M. tuberculosis* involves the generation of mycobacteria-specific T cells and the formation of protective granulomas [2, 3]. Protective granulomas are compact structures where infected macrophages are interspersed with lymphocytes that form cuffs around the macrophages or wedges between monocytic cells [2, 4]. Although initially effective at containing *M. tuberculosis* infection, the granulomas can grow and erode into bronchi leading to cavities and dissemination of infection [2, 5]. Understanding how the immune system regulates inflammation and granuloma formation against *M. tuberculosis* may help design more effective therapies to limit the damaging inflammation that is characteristic of TB disease.

Roquin is an E3 ligase involved in immune regulation and is essential for the maintenance of T cell tolerance [6, 7]. Roquin deficiency is lethal, demonstrating the essential nature of this ligase in controlling development [8, 9]. In *sanroque* mice, a single point mutation in *Roquin1/Rc3rh1* leads to ICOS and IFN-γ upregulation by *sanroque* T cells [6, 7]. As a result of this mutation, these mice accumulate increased numbers of T follicular helper (T_{FH}) cells and develop autoimmune disease [6, 7]. Roquin is a RNA binding protein and has demonstrated roles in regulating expression of ICOS, IFN-γ and OX40 amongst other targets, T cell activation and T_{FH} cell function [6–8, 10]. To date, the role of Roquin in regulating immunity to bacterial pathogens has not been examined. Using young *sanroque* mice, the current study demonstrates that a mutation in Roquin affects both the T cell-mediated immune response and the granulomatous response to *M. tuberculosis* infection and demonstrates how these factors contribute to the overall control of *M. tuberculosis* infection.

Materials and Methods

Mice

C57BL/6 wild-type (WT) and *Rag1*-deficient (*Rag1*$^{-/-}$) mice (Animal Resources Centre (Perth, Australia) and *Roquin1/Rc3h1* (*sanroque*, *Roquin*$^{san/san}$) [6] and *sanroque.Rag1*$^{-/-}$ mice, bred and maintained in the Centenary Institute Animal facility, were used at 6 weeks. P25 CD4^{+} TCR-transgenic (Tg) mice specific for amino acids 240-254 of *M. tuberculosis* Ag85B were provided by Prof. K. Takatsu [11] (Nihon University, Tokyo, Japan) and Dr. J. Ernst (New York University, NY). All scientific studies using these mice were approved by the Animal care and Ethics Committee, University of Sydney, Sydney, Australia or the Sydney Local Health District under protocol numbers: K75/9-2010/3/5387, K75/3-2007/3/4561 and AEC2013-063.

Mycobacteria and infections

M. tuberculosis H37Rv and *M. bovis* Bacille Calmette-Guérin (BCG) were cultured in Middlebrook 7H9 broth (Difco Laboratories, Detroit, MI) supplemented with 10% albumin-dextrose-catalase (ADC) and stored at -70 ºC. WT, *sanroque*, *Rag1*$^{-/-}$ and *sanroque.Rag1*$^{-/-}$

mice were infected via aerosol with ~100 colony forming units (CFU) of *M. tuberculosis* H37Rv using a Middlebrook airborne infection apparatus (Glas-Col, Terre Haute, IN, USA) or intravenously (I.V.) with 10^4 CFU of *M. tuberculosis* H37Rv. Bacterial growth were quantitated by plating serial dilution of organ homogenates or bone marrow derived (BMd) macrophages lysed with 200 μL of 0.01% triton-X100 on Middlebrook 7H11 agar (BD) at 37 ºC for 2-3 weeks.

Antigen used for cell stimulation

Culture filtrate protein (CFP) containing excreted and secreted proteins from *M. tuberculosis* H37Rv [12] was obtained from the Biodefense and Emerging Infections Research Resources repository, USA.

Lung images and involvement

Organs were fixed in 10% neutral buffered formalin, paraffin embedded and sectioned at 5 μm and H&E stained by Histopathology, Veterinary Pathology Diagnostic Services, University of Sydney. An image of each entire lung lobe was taken at 10X magnification on a Leica DM6000B microscope. The threshold of the image was set in Adobe Photoshop, such that the lung parenchyma appeared white and areas of inflammation black and pixilation was recorded at this point as A. The threshold was then changed to blacken the entire lobe and the level of pixilation was recorded as B. The percentage of lung involvement = (A/B) x 100 [13].

Single cell suspensions

Lungs were digested in collagenase I and DNase I in RPMI media at 37 ºC for 30 mins. Lung cells were dispersed through a 70 μm nylon sieve, red blood cells lysed with ACK lysis buffer for 30 seconds. Lymph nodes (LNs) were also process through a sieve to obtain single cell suspensions. Spleens harvested from P25 TCR-Tg mice were processed through a sieve and red blood cells were lysed for 1 min.

BMd macrophages were prepared as previously described [14]. After 5 days culture they were stimulated overnight with 100 U IFN-γ (R&D systems USA) then infected with *M. bovis* BCG, extracellular bacteria was removed after 4 hours and bacterial viability assessed at 24 hours as previous described [14]. Cytokine levels were measured by CBA and Nitric Oxide by Greiss reaction.

Flow cytometry

Mediastinal lymph node (MLN) and lung cells (~4 x10^5-10^6/well) were preincubated with Fc block (2.4G2, BD Bioscience) for 10 mins at 4 °C, before staining with the antibodies detailed below in FACS wash at 4 °C for 15 mins, before cells were washed and fixed in 10% neutral buffered formalin. For intracellular cytokine staining, cells were stimulated with CFP (10 μg/mL) overnight then treated with Brefeldin A (10 μg/mL) (Sigma-Aldrich) for 4 hours prior to staining. Cells were stained for surface markers as described above, then fixed and permeablised for 20 mins at RT with 100 μL per sample of Cytofix/Cytoperm buffer (BD Biosciences) and washed with Cytowash (BD Biosciences). Anti-cytokine antibodies were diluted in Cytowash and incubated with the cells at 4 °C for 20 mins. The cells were

washed twice with Cytowash and suspended in 10% neutral buffered formalin. Antibodies used were; CD4-AF700 & PE-Cy7 (RM4-5, BD Biosciences), CD8-PerCP & APC-Cy7 (53-6.7, BD Biosciences), ICOS-PE (7E.17G9, eBioscience), CXCR5-PE-Cy7 (2G8, BD Biosciences), CD45.2-Pacific Blue (104, Biolegend), CD44-FITC (IM7, BD Biosciences), CD62L-APC-Cy7 (MEL-14, Biolegend), IFN-γ-FITC (XMG1.2 BD Biosciences), TNF-APC & PE (MP6-XT22, Biolegend) and Live/Dead Blue reactive dye (BD Biosciences). LSR II or LSR Fortessa flow analysers (BD Bioscience) were used to acquire the samples and FlowJo analysis software (Tree Star) used to analyse the samples. The gating strategies are outlined in Supplementary figure 4.

Cytokine bead array

CXCL1 (KC), CCL5 (RANTES), CCL3 (MIP-1α) and CCL2 (MCP-1) in clarified lung homogenates (homogenised lungs were spun at 3200 g for 10 mins at RT), or IL-1 and TNF from BMd macrophage cultures were measured by cytometric bead assay (CBA) (BD Biosciences) as per the manufacturer's instructions. Samples were acquired using the LSR Fortessa or LSR II and analysed using the FCAP software (BD Biosciences).

Transfer of *M. bovis* BCG-primed T cells into *Rag1*$^{-/-}$ mice

WT and *sanroque* mice were immunised subcutaneously with 5 x 10^5 CFU of *M. bovis* BCG at the base of tail and in both footpads. 21 days post immunization draining LNs (inguinal, popliteal and Para-aortic) were digested in complete RPMI 1640 (Invitrogen) with 5 U/ml collagenase (Boehringer) and 13 μg/ml DNase1 (Worthington) for 30 mins at 37 °C. Single cell suspensions were cultured in media (10^6 cells/ml) with *M. bovis* BCG sonicate (10 μg/ml) and recombinant IL-2 (2 ng/ml) (R&D Systems) for 8 days. *M. bovis* BCG sonicate was prepared by 3X 1 min sonication at 60% amplitude (BRANSON digital Sonifier). On day 8, 2.5 x 10^6 cultured cells and 1 x 10^4 bacilli of *M. tuberculosis* H37Rv were injected I.V. into *Rag1*$^{-/-}$ mice. 18 days following infection, lung, liver and spleen were homogenized and plated on 7H11 agar to assess bacterial growth.

Transfer of P25 TCR-Tg spleen cells into *Rag1*$^{-/-}$ mice

Purified spleen cells (2 x 10^6) harvested from P25 TCR-Tg mice, were injected I.V. into WT.*Rag1*$^{-/-}$ and *sanroque*.*Rag1*$^{-/-}$ mice challenged with an aerosol infection with *M. tuberculosis* H37Rv on the following day.

Statistical Analysis

Statistical differences were analysed in Prism (GraphPad Software), with one-way analysis of variance (ANOVA) with Tukey's multiple comparison test used for comparison of multiple samples, or unpaired Student's *t* tests for two samples. The differences with $p<0.05$ were considered significant.

Results

Increased T cell activation and mycobacteria-specific cytokine production during *M. tuberculosis* infection in *sanroque* mice

Roquin is involved in immune tolerance, however its role in immunity to bacterial infections is not clear. *Sanroque* mice, homozygous for a point mutation in the *Roquin1* gene, were infected by aerosol with low dose *M. tuberculosis* to examine the effect of Roquin on the immune response against *M. tuberculosis*. As the *sanroque* mice progressively develop an autoimmune disease, mice were utilized at 6 weeks of age. Previous studies have shown that as a result of their autoimmune conditions *sanroque* mice have enlarged lymph nodes and spleens, with increased numbers of activated ($CD44^{Hi}CD62^{Low}$) $CD4^+$ and $CD8^+$ T cells and T_{FH} cells from 6-7 weeks of age which accumulate as they age [6]. In this study the MLNs of *sanroque* mice, regardless of infection, were larger than the WT mice, with increased numbers of activated $CD4^+$ T cells in the MLNs at all time points (including uninfected *sanroque* mice) (Fig 1A-D). WT mice show increased accumulation of cells in MLN as infection progressed (Fig 1A-D). Similarly, lungs of WT mice show increased accumulation of activated T cells that peaked at 4 weeks and were maintained at 8 weeks, while *sanroque* mice continue to show increased recruitment of activated T cells into the lungs up to 8 weeks (Fig 1A-D). The numbers of T_{FH} cells ($CD4^+CXCR5^+ICOS^+$) showed a similar pattern of recruitment (Fig 1E-H) with *sanroque* mice showing increased accumulation of T_{FH} cells into the lung at 8 weeks post-infection.

To examine mycobacterial-antigen specific cytokine responses, T cells were restimulated with CFP [15]. Early in infection TNF producing $CD4^+$ and $CD8^+$ T cells were evident in the lung and MLN of both WT and *sanroque* mice though the percentage of these cells were significantly higher in the *sanroque* mice (Fig 2A and 2B). At 4 weeks, which was the peak of the bacterial load in the WT mice (Fig 3), these mice showed a significantly higher percentage of IFN-γ producing $CD4^+$ T cells in the lung, compared to the *sanroque* mice (Fig 2C & D). The *sanroque* mice still showed significantly higher percentages of TNF producing $CD4^+$ and $CD8^+$ T cells, but only in the MLN. By 8 weeks, when *sanroque* mice show increased bacterial burden in the lung, this was accompanied by an increase in the percentage of IFN-γ producing T cells in the MLN and lung compared to WT infected mice (Fig 2E and F), which may have been driven by the rising antigenic load (Fig 3). The percentage of IL-17^+ $CD4^+$ and $CD8^+$ T cells was low in both strains of mice throughout the infection, though by 8 weeks there was a significantly higher percentage of $CD8^+$ IL-17 producing T cells in the MLN of the *sanroque* mice compared to the WT mice.

Sanroque mice control early but not late *M. tuberculosis* infection

Two weeks following aerosol infection, *sanroque* mice showed delayed bacterial dissemination into the spleen compared to WT littermates (Fig 3A). From 4 experiments, 14/15 *sanroque* mice had no detectable bacteria in the spleen while 11/16 WT mice showed dissemination to the spleen by this time (Sup. Fig 1). The increase in activated T cells (Fig 1) and the enhanced TNF response (Fig 2) was associated with a significant delay in dissemination consistent with the control of bacterial growth. However, by 4 weeks post-infection both groups of mice showed equivalent bacterial loads (Fig 3A), and as the

infection progressed to a chronic stage, *sanroque* mice demonstrated reduced ability to control infection in the lung (Fig 3A). Interestingly, bacterial growth in the spleen remained significantly lower in the *sanroque* mice (Fig 3A). Furthermore, this increase in bacterial growth in the lung was associated with dysregulated inflammation (Fig 3B). *Sanroque* mice developed larger lesions with granulomas that lacked the organized structure seen in WT mice (Fig 3B). WT mice granulomas showed dense areas of lymphocytes cuffing the macrophages while those in *sanroque* mice contained large lesions, composed predominantly of macrophages with less dense infiltration of lymphocytes (Fig 3B). These lymphocytic cuffs are likely composed of both T and B lymphocytes [16, 17]. Interestingly at 8 weeks post-infection, WT but not *sanroque* mice showed increased recruitment of B cells into the lungs (Sup. Fig 2E). These findings demonstrate an important role for Roquin in regulating the inflammatory response to *M. tuberculosis* infection. To examine how Roquin functions at the cellular level we examined the role of Roquin in different immune cell subsets.

Transfer of antigen-specific *sanroque* T cells protects against *M. tuberculosis* infection with reduced inflammation

At 8 weeks post-*M. tuberculosis* infection, *sanroque* mice showed increased bacterial growth in the lung with dysregulated granuloma formation. To examine whether a defect in the activation of antigen-specific T cells was responsible for this, we measured the protective efficacy of *sanroque* T cells independent of other Roquin mutated cells. *M. bovis* BCG-primed *sanroque* T cells were transferred into *Rag1*$^{-/-}$ recipient mice that were then infected systemically with *M. tuberculosis*. In this model, mice were infected I.V. to provide sufficient antigen to stimulate the transferred T cells [18]. The transfer of T cells from either WT or *sanroque M. bovis* BCG-immunised mice reduced the growth of *M. tuberculosis* in the spleen, liver and lung compared to *Rag1*$^{-/-}$ mice receiving T cells from unimmunised mice (Fig 4A-C). In the spleen and liver the transfer of T cells from unimmunised mice, either WT or s*anroque*, was sufficient to reduce *M. tuberculosis* growth compared to *Rag1*$^{-/-}$ mice alone, though in the lung, only the transfer of T cells from immunised WT mice provided significant protection compared to infected *Rag1*$^{-/-}$ mice. The transfer of T cells from immunised *sanroque* mice reduced bacterial growth however this did not reach significance by ANOVA**.** What was striking about the response of mice receiving T cells from immunised *sanroque* mice was the significant reduction in inflammation in the lungs compared with the *Rag1*$^{-/-}$ mice receiving T cells from immunised WT mice (Fig 4D) despite the fact that they had higher bacterial loads (Fig 4C). These lesions were macrophage dominant with the lymphocytes localised around the perivascular region. This differed from the response seen in *M. tuberculosis* infected WT mice described in Figure 3B, which showed granulomas with lymphocyte aggregates surrounding the monocytes/macrophages. Interestingly the *Rag1*$^{-/-}$ receiving T cells from unimmunised *sanroque* mice also displayed a trend towards reduced lung inflammatory involvement though this did not reach significance. This study demonstrates that mycobacteria-specific T cells generated in the absence of normal Roquin can stimulate control of mycobacterial infection.

Transfer of mycobacteria-specific T cells enhances control of *M. tuberculosis* infection in *sanroque.Rag1*$^{-/-}$ mice

The dysregulated inflammatory response seen in the lungs of *sanroque* mice during chronic *M. tuberculosis* infection may have been influenced by the development of autoimmune conditions common in *sanroque* mice [6, 7]. To examine the functions of the Roquin mutation in myeloid cells in the absence of this autoimmune complication, *sanroque.Rag1*$^{-/-}$ mice were used [19]. Mycobacteria-specific splenic cells from P25 TCR-Tg mice [11] were transferred into *sanroque.Rag1*$^{-/-}$ or *Rag1*$^{-/-}$ controls, then infected with a low dose aerosol of *M. tuberculosis* to mimic the a natural route of infection. Interestingly, at 8 weeks post-infection the transfer of P25 spleen cells into *sanroque.Rag1*$^{-/-}$ mice enhanced control of bacterial growth in the lung compared to *Rag1*$^{-/-}$ control mice receiving the same number of P25 spleen cells (Fig 5A-B), though similar numbers of activated T cells were recovered from the lungs of both groups of mice (Fig 5D-E).

This reduced bacterial load was associated with significantly reduced inflammation in the lungs of these *sanroque.Rag1*$^{-/-}$ mice (Fig 6A). Therefore we examined if the Roquin mutation influenced the recruitment of myeloid cells into the lungs of the infected *Rag1*$^{-/-}$ mice (Fig 6). At 2 weeks post-infection, both WT.*Rag1*$^{-/-}$ and *sanroque.Rag1*$^{-/-}$ mice had similar numbers of CD45.2^{+} cells in the lungs, by 8 weeks there was a trend towards increased recruitment of CD45.2^{+} cells to the lungs of WT.*Rag1*$^{-/-}$ mice but this did not reach significance (Fig 6B). Equivalent numbers of neutrophils (CD11b^{Hi}Ly6G^{Hi}) were seen at both time points (Fig 6B). At 2 weeks WT and *sanroque.Rag1*$^{-/-}$ mice had equivalent numbers of alveolar macrophages (CD11b$^{Low\text{-}Mid}$CD11c^{Hi}), DCs (CD11b^{Hi}CD11c^{Hi}) and monocytes/macrophages (CD11b$^{Mid\text{-}Hi}$CD11c$^{Low\text{-}Mid}$) (data not shown), however by 8 weeks the numbers of monocytes/macrophages were significantly reduced in the *sanroque.Rag1*$^{-/-}$ mice (Fig 6B). This reduction was associated with significantly lower levels of the leucocyte recruiting chemokines MIP-1β and RANTES in the lungs (Fig 7). When we examined the cytokine response of the resident CD45.2^{+} *Rag1*$^{-/-}$ myeloid cells, the WT.*Rag1*$^{-/-}$ mice cells initially showed increased percentages of TNF-producing CD11b$^{Low\text{-}Mid}$ and CD11b^{Hi} cells compared to the *sanroque.Rag1*$^{-/-}$ mice that received P25 spleen cells, whereas by 8 weeks, these *sanroque.Rag1*$^{-/-}$ showed a higher percentage of TNF-producing CD11b^{Hi} cells (Fig 6B). Similarly BMd *sanroque* macrophages were able to control mycobacteria as effectively as WT macrophages, despite inducing less TNF (Sup. Fig 3).

These findings identify complex multiple roles of Roquin in regulating immune cell function during *M. tuberculosis* infection and reveal that it is possible to both enhance control of mycobacterial growth and to limit the lung-damaging pathology often associated with *M. tuberculosis* infection.

Discussion

The E3 ubiquitin ligase, Roquin, is involved in immune regulation, influencing both T cell and myeloid cell functions [6]. These studies demonstrate that Roquin plays a role in regulating the inflammatory response against *M. tuberculosis*, aiding in the formation of protective granulomas and importantly, maintaining control of chronic infection. Results

with the *sanroque.Rag1*$^{-/-}$ mice suggest that the function of Roquin differs depending upon the immune cell examined and that normal Roquin in myeloid cells, actually contributes to the increased inflammatory cell influx and damaging pathology associated with TB disease.

In TB patients, upregulated ICOS expression has been correlated with induction of protective Th1 responses, with increased IFN-γ release from T cells [20]. S*anroque* mice have increased numbers of activated T cells with enhanced ICOS, TNF and IFN-γ expression [6] and this was associated with early containment of the TB infection at 2 weeks. At 4 weeks, the frequencies of IFN-γ, TNF and IL-17 producing T cells were similar in both strains of mice as were the bacterial loads. By 8 weeks, contrary to expectations, despite the increase in T cell activation, ICOS expression and mycobacteria-specific IFN-γ^{+} T cells did not equate with enhanced protection in the *Sanroque* mice. Repeated studies have demonstrated that while IFN-γ is essential for protective immunity against *M. tuberculosis* [21, 22], increased IFN-γ production does not necessarily correlate with increased protection [23–25]. Indeed the increase in bacterial load in the lungs of the *Sanroque* mice at this time may have driven the increase in IFN-γ and TNF producing T cells. Identifying appropriate correlates of protection would greatly assist in assessing the effects of new vaccines or drug treatments.

The Roquin mutation also gives rise to T_{FH} cell accumulation [6]. The influence of T_{FH} cells on immunity to *M. tuberculosis* infection is not well understood. Uninfected *sanroque* mice had increased numbers of T_{FH} cells in the lung compared to WT mice, and this was further enhanced by *M. tuberculosis* infection. T_{FH} cells express CXCR5, and Slight *et al.* demonstrated a role for CXCR5^{+} CD4^{+} T cells in orchestrating the spatial arrangement of T cells in *M. tuberculosis* induced granulomas [26]. *M. tuberculosis* infected *Cxcr5*$^{-/-}$ mice lacked the ectopic lymphoid structures present in WT mice, suggesting that CXCR5^{+} T cells, which include T_{FH} cells, are involved in formation of lymphoid follicles in the lung during TB infection [26]. Our data demonstrates that increased numbers of T_{FH} cells, as seen in our *sanroque* mice, did not enhance protective granuloma formation in the lung during *M. tuberculosis* infection.

Protective granuloma formation is essential to maintain immunity to *M. tuberculosis* [27]. A feature of protective granulomas includes formation of dense aggregates of lymphocytes, also referred to as lymphocytic cuffing [3]. *Sanroque* mice lacked the lymphocytic aggregations surrounding the centralised infected mononuclear cells evident in WT mice. One explanation for the failure to contain infection is that the impaired localisation of lymphocytes, including *M. tuberculosis*-specific T cells, may have limited the interactions with infected macrophages that are necessary to contain bacterial growth. The lack of lymphocyte aggregation may also be influenced by the reduced accumulation of B cells in the lungs of the *sanroque* mice. Studies using B cell knockout mice indicate that B cells play a role in forming and maintaining the dense lymphocytic aggregates usually evident in *M. tuberculosis* induced granulomas [16, 17, 28]. Maintaining the structural integrity of granulomas is essential to control *M. tuberculosis* growth. Mice with defects in the formation of granulomas such as *Tnf*$^{-/-}$ mice are extremely susceptibility to infection despite mounting strong antigen-specific immune responses [29].

TNF is essential for normal granuloma formation. The Roquin mutation has been associated with enhanced TNF secretion [19, 30]. Knock down of Roquin using siRNA in the macrophage like cell-line RAW264.7, prevented decay of *tnf* mRNA transcripts and increased membrane bound and secreted TNF [30]. Another study [19] demonstrated that *sanroque.Rag1*$^{-/-}$ mice were more susceptible to serum induced experimental arthritis, which was diminished in *sanroque.Rag1*$^{-/-}$ x TNF$^{-/-}$ mice [19] suggesting that the Roquin mutation in myeloid cells increased TNF expression. Both excessive and inhibited TNF production in murine infectious models can result in uncontrolled inflammation [29, 31, 32]. In this study the effect of the Roquin mutation on TNF production was influenced both by the mycobacterial infection and the cell type involved. *Sanroque* mice had increased percentages of TNF producing T cells, particularly early in infection. While in *sanroque.Rag1*$^{-/-}$ mice following transfer of P25 splenic cells, the level of TNF producing CD11b^{+} cells actually decreased early in infection compared to *WT.Rag1*$^{-/-}$ mice without compromising control of infection. Similarly, BMd macrophages from *sanroque* mice controlled bacterial growth but interestingly produced less TNF than WT infected macrophages, suggesting that it is possible to reduce the inflammatory response induced by *M. tuberculosis* infection without compromising containment of mycobacterial infection.

One difficulty with studying *sanroque* mice is their propensity to develop the autoimmune disease SLE, which is accompanied by glomerulonephritis in mice as well as humans [6, 33]. Renal failure impairs cellular immune responses and increases susceptibility to infection [34, 35], and the incidence of TB is higher in patients with chronic renal disease in TB endemic countries [34, 35]. The development of autoimmune renal disease in aging *sanroque* mice may have rendered these mice more susceptible to chronic *M. tuberculosis* infection. To compensate for this we examined the role of Roquin in specific immune cell subsets. Transferring T cells from *M. bovis* BCG-immunised and unimmunised mice into *Rag1*$^{-/-}$ mice demonstrated that the presence of the Roquin mutation did not impair the generation of mycobacteria-specific T cells nor their ability to reduce mycobacterial growth compared to the transfer of naïve T cells. Most interestingly, the transfer of mycobacteria-specific spleen cells (WT Roquin) into *sanroque.Rag1*$^{-/-}$ mice actually resulted in increased protection against *M. tuberculosis* infection with significantly lower bacterial loads at 8 weeks compared to similarly treated *Rag1*$^{-/-}$ control mice, reduced chemokines and reduced numbers of macrophages in the lungs, and markedly reduced inflammatory involvement and immunopathology. The reduced chemokines found in *sanroque.Rag1*$^{-/-}$ mice may be a consequence of the reduced antigenic load leading to the stimulation of fewer cells, or alternatively the reduced chemokine expression may have led to lower cellular infiltrate. Importantly, during *M. tuberculosis* infection myeloid cells in *sanroque.Rag1*$^{-/-}$ mice induced sufficient inflammatory responses to recruit the necessary cells into the lungs and contain infection. In TB infection protecting against the pathogen, but limiting the immune-mediated pathology is essential [31]. Several studies have demonstrated that enhanced protection against mycobacterial infection is often associated with limited lung pathology [31, 36] as is the case in the *sanroque.Rag1*$^{-/-}$ mice in this study.

Roquin regulates the function of key immune cells including T cells, B cells and myeloid cells [37]. Roquin may exert its effects either as an RNA binding protein or through its E3 ubiquitin ligase activity [38] and both of these mechanisms may contribute to protective

immunity. The binding of Roquin to its target mRNA is known to facilitate the degradation of transcripts from multiple immune genes including *Icos*, *Il6*, *Tnf* and *Irf4* [6, 10, 19, 37], all of which have critical roles in regulating host immunity to *M. tuberculosis*. The E3 ligase activity of Roquin has not been well described [38], but other E3 ligases have been shown to be important in protection against mycobacterial infections. Genetic variations in the E3 ligase genes, *PARK2* and *UBE3A*, are associated with increased susceptibility to the mycobacterial infections, leprosy and TB respectively, in humans [39–41]. The *PARK2* gene encodes the protein Parkin, and a recent study demonstrated that Parkin targets *M. tuberculosis*-containing phagosomes, resulting in increased autophagy-mediated killing of *M. tuberculosis* within macrophages [40]. Similarly to Parkin, Roquin may also be involved in autophagy. Further study of the mutated Roquin in myeloid cells may provide new insights into increasing mycobacteriocidal capacity of myeloid cells to limit the lung pathology associated with *M. tuberculosis* infection.

In summary, this study has demonstrated the complex roles Roquin plays in the control of *M. tuberculosis* infection, depending upon the stage of infection and cell type involved. Importantly they demonstrate roles for Roquin in enhancing mycobacterial growth and the lung-damaging pathology often associated with *M. tuberculosis* infection.

Supplementary Material

Refer to Web version on PubMed Central for supplementary material.

Acknowledgments

We thank Paul Reynold, Tuyet Tran and Theresa Corpus for technical support.

This work was supported by NHMRC project grant (APP#570771), Wellcome Trust Strategic Award. GN was supported by a University of Sydney Postgraduate Award.

References

1. World Health Organisation. Gobal Tuberculosis Report 2016. World Health Organization; Geneva: 2016.
2. Ehlers S, Schaible UE. The granuloma in tuberculosis: Dynamics of a host-pathogen collusion. Front Immunol. 2013; 3:1–9. 411.
3. Saunders BM, Britton WJ. Life and death in the granuloma: immunopathology of tuberculosis. Immunol Cell Biol. 2007; 85:103–111. [PubMed: 17213830]
4. Silva Miranda M, Breiman A, Allain S, Deknuydt F, Altare F. The tuberculous granuloma: an unsuccessful host defence mechanism providing a safety shelter for the bacteria? Clin Dev Immunol. 2012; 2012:1–14. Article ID 139127.
5. Harper J, Skerry C, Davis SL, Tasneen R, Weir M, Kramnik I, Bishai WR, Pomper MG, Nuermberger EL, Jain SK. Mouse Model of Necrotic Tuberculosis Granulomas Develops Hypoxic Lesions. J Infect Dis. 2012; 205:595–602. [PubMed: 22198962]
6. Vinuesa CG, Cook MC, Angelucci C, Athanasopoulos V, Rui L, Hill KM, Yu D, Domaschenz H, Whittle B, Lambe T, Roberts IS, et al. A RING-type ubiquitin ligase family member required to repress follicular helper T cells and autoimmunity. Nature. 2005; 435:452–458. [PubMed: 15917799]
7. Di Y, Tan AH-M, Hu X, Athanasopoulos V, Simpson N, Silva DG, Hutloff A, Giles KM, Leedman PJ, Lam KP, Goddnow CC, et al. Roquin represses autoimmunity by limiting inducible T-cell co-stimulator messenger RNA. Nature. 2007; 450:299–303. [PubMed: 18172933]

8. Vogel, Katharina U., Edelmann, Stephanie L., Jeltsch, Katharina M., Bertossi, A., Heger, K., Heinz, Gitta A., Zöller, J., Warth, Sebastian C., Hoefig, Kai P., Lohs, C., Neff, F., et al. Roquin paralogs 1 and 2 redundantly Repress the Icos and Ox40 costimulator mRNAs and control follicular helper T cell differentiation. Immunity. 2013; 38:655–668. [PubMed: 23583643]
9. Bertossi A, Aichinger M, Sansonetti P, Lech M, Neff F, Pal M, Wunderlich FT, Anders H-J, Klein L, Schmidt-Supprian M. Loss of Roquin induces early death and immune deregulation but not autoimmunity. J Exp Med. 2011; 208:1749–1756. [PubMed: 21844204]
10. Lee, Sau K., Silva, Diego G., Martin, Jaime L., Pratama, A., Hu, X., Chang, P-P., Walters, G., Vinuesa, CG. Interferon-γ excess leads to pathogenic accumulation of follicular helper T cells and germinal centers. Immunity. 2012; 37:880–892. [PubMed: 23159227]
11. Tamura T, Ariga H, Kinashi T, Uehara S, Kikuchi T, Nakada M, Tokunaga T, Xu W, Kariyone A, Saito T, Kitamura T, et al. The role of antigenic peptide in $CD4^+$ T helper phenotype development in a T cell receptor transgenic model. Int Immunol. 2004; 16:1691–1699. [PubMed: 15477229]
12. Målen H, Søfteland T, Wiker HG. Antigen analysis of *Mycobacterium tuberculosis* H37Rv Culture Filtrate Proteins. Scand J Immunol. 2008; 67:245–252. [PubMed: 18208443]
13. Saunders BM, Tran S, Ruuls S, Sedgwick JD, Briscoe H, Britton WJ. Transmembrane TNF Is Sufficient to Initiate Cell Migration and Granuloma Formation and Provide Acute, but Not Long-Term, Control of *Mycobacterium tuberculosis* Infection. J Immunol. 2005; 174:4852–4859. [PubMed: 15814712]
14. Blumenthal A, Nagalingam G, Huch JH, Walker L, Guillemin GJ, Smythe GA, Ehrt S, Britton WJ, Saunders BM. *M. tuberculosis* induces potent activation of IDO-1, but this is not essential for the immunological control of infection. PLoS ONE. 2012; doi: 10.1371/journal.pone.0037314
15. Andersen P, Askgaard D, Ljungqvist L, Bennedsen J, Heron I. Proteins released from *Mycobacterium tuberculosis* during growth. Infect Immun. 1991; 59:1905–1910. [PubMed: 1903768]
16. Maglione PJ, Chan J. How B cells shape the immune response against *Mycobacterium tuberculosis*. Eur J Immunol. 2009; 39:676–686. [PubMed: 19283721]
17. Maglione PJ, Xu J, Chan J. B Cells Moderate Inflammatory progression and enhance bacterial containment upon pulmonary challenge with *Mycobacterium tuberculosis*. J Immunol. 2007; 178:7222–7234. [PubMed: 17513771]
18. Wozniak TM, Saunders BM, Ryan AA, Britton WJ. *Mycobacterium bovis* BCG-Specific Th17 cells confer partial protection against *Mycobacterium tuberculosis* infection in the absence of gamma interferon. Infect Immun. 2010; 78:4187–4194. [PubMed: 20679438]
19. Pratama A, Ramiscal Roybel R, Silva Diego G, Das Souvik K, Athanasopoulos V, Fitch J, Botelho Natalia K, Chang P-P, Hu X, Hogan Jennifer J, Jennifer J, et al. Roquin-2 shares functions with its paralog Roquin-1 in the repression of mRNAs controlling T follicular helper cells and systemic inflammation. Immunity. 2013; 38:669–680. [PubMed: 23583642]
20. Quiroga MF, Pasquinelli V, Martinez GJ, Jurado JO, Zorrilla LC, Musella RM, Abbate E, Sieling PA, Garcia VE. Inducible costimulator: a modulator of IFN-gamma production in human tuberculosis. J Immunol. 2006; 176:5965–5974. [PubMed: 16670305]
21. Pearl JE, Saunders BM, Ehlers S, Orme IM, Cooper AM. Inflammation and lymphocyte activation during mycobacterial infection in the interferon-gamma-deficient mouse. Cell Immunol. 2001; 211:43–50. [PubMed: 11585387]
22. Flynn JL, Chan J, Triebold K, Dalton DK, Stewart TA, Bloom BR. An essential role for interferon-γ in resistance to *Mycobacterium tuberculosis* infection. J Exp Med. 1993; 178:2249–2254. [PubMed: 7504064]
23. Hoft DF, Worku S, Kampmann B, Whalen CC, Ellner JJ, Hirsch CS, Brown RB, Larkin R, Li Q, Yun H, Silver RF. Investigation of the relationships between immune-mediated inhibition of mycobacterial growth and other potential surrogate markers of protective *Mycobacterium tuberculosis* Immunity. J Infect Dis. 2002; 186:1448–1457. [PubMed: 12404160]
24. Elias D, Akuffo H, Britton S. PPD induced in vitro interferon gamma production is not a reliable correlate of protection against *Mycobacterium tuberculosis*. Trans R Soc Trop Med Hyg. 2005; 99:363–368. [PubMed: 15780343]

25. Kamath AT, Hanke T, Briscoe H, Britton WJ. Co-immunization with DNA vaccines expressing granulocyte–macrophage colony-stimulating factor and mycobacterial secreted proteins enhances T-cell immunity, but not protective efficacy against *Mycobacterium tuberculosis*. Immunology. 1999; 96:511–516. [PubMed: 10233735]
26. Slight SR, Rangel-Moreno J, Gopal R, Lin Y, Fallert Junecko BA, Mehra S, Selman M, Becerril-Villanueva E, Baquera-Heredia J, Pavon L, Kaushal D, et al. CXCR5^{+} T helper cells mediate protective immunity against tuberculosis. J Clin Invest. 2013; 123:712–726. [PubMed: 23281399]
27. Saunders BM, Frank AA, Orme IM. Granuloma formation is required to contain bacillus growth and delay mortality in mice chronically infected with *Mycobacterium tuberculosis*. Immunology. 1999; 98:324–328. [PubMed: 10583589]
28. Torrado E, Fountain JJ, Robinson RT, Martino CA, Pearl JE, Rangel-Moreno J, Tighe M, Dunn R, Cooper AM. Differential and site specific impact of B cells in the protective immune response to *Mycobacterium tuberculosis* in the mouse. PLoS ONE. 2013; doi: 10.1371/journal.pone.0061681
29. Bean AGD, Roach DR, Briscoe H, France MP, Korner H, Sedgwick JD, Britton WJ. Structural deficiencies in granuloma formation in TNF gene-targeted mice underlie the heightened susceptibility to aerosol *Mycobacterium tuberculosis* infection, which is not compensated for by lymphotoxin. J Immunol. 1999; 162:3504–3511. [PubMed: 10092807]
30. Leppek K, Schott J, Reitter S, Poetz F, Hammond MC, Stoecklin G. Roquin promotes constitutive mRNA decay via a conserved class of stem-Loop recognition motifs. Cell. 2013; 153:869–881. [PubMed: 23663784]
31. Bekker L-G, Moreira AL, Bergtold A, Freeman S, Ryffel B, Kaplan G. Immunopathologic effects of tumor necrosis factor alpha in murine mycobacterial infection are dose dependent. Infect Immun. 2000; 68:6954–6961. [PubMed: 11083819]
32. Saunders BM, Briscoe H, Britton WJ. T cell-derived tumour necrosis factor is essential, but not sufficient, for protection against *Mycobacterium tuberculosis* infection. Clin Exp Immunol. 2004; 137:279–287. [PubMed: 15270844]
33. Bagavant H, Fu SM. Pathogenesis of kidney disease in systemic lupus erythematosus. Curr Opin Rheumatol. 2009; 21:489–494. [PubMed: 19584729]
34. Li SY, Chen TJ, Chung KW, Tsai LW, Yang WC, Chen JY, Chen TW. *Mycobacterium tuberculosis* infection of end-stage renal disease patients in Taiwan: a nationwide longitudinal study. Clin Microbiol Infect. 2011; 17:1646–1652. [PubMed: 21375664]
35. Rutsky EA, Rostand SG. Mycobacteriosis in patients with chronic renal failure. Arch Intern Med. 1980; 140:57–61. [PubMed: 7352805]
36. Bourigault M-L, Vacher R, Rose S, Olleros ML, Janssens J-P, Quesniaux VFJ, Garcia I. Tumor necrosis factor neutralization combined with chemotherapy enhances *Mycobacterium tuberculosis* clearance and reduces lung pathology. Am J Clin Exp Immunol. 2013; 2:124–134. [PubMed: 23885330]
37. Athanasopoulos V, Ramiscal RR, Vinuesa CG. Roquin signalling pathways in innate and adaptive immunity. Eur J Immunol. 2016; 46:1082–1090. [PubMed: 27060455]
38. Zhang Q, Fan L, Hou F, Dong A, Wang YX, Tong Y. New insights into the RNA-binding and E3 ubiquitin ligase activities of Roquins. Sci Rep. 2015; 5:1–13. 15660.
39. Cervino ACL, Lakiss S, Sow O, Bellamy R, Beyers N, Hoal-van HE, van Helden P, McAdam KPWJ, Hill AVS. Fine mapping of a putative tuberculosis-susceptibility locus on chromosome 15q11–13 in African families. Hum Mol Gen. 2002; 11:1599–1603. [PubMed: 12075004]
40. Manzanillo PS, Ayres JS, Watson RO, Collins AC, Souza G, Rae CS, Schneider DS, Nakamura K, Shiloh MU, Cox JS. The ubiquitin ligase parkin mediates resistance to intracellular pathogens. Nature. 501:512–516.
41. Mira MT, Alcais A, Van Thuc N, Moraes MO, Di Flumeri C, Hong Thai V, Chi Phuong M, Thu Huong N, Ngoc Ba N, Xuan Khoa P, Sarno EN, et al. Susceptibility to leprosy is associated with PARK2 and PACRG. Nature. 2004; 427:636–640. [PubMed: 14737177]

Europe PMC Funders Author Manuscripts

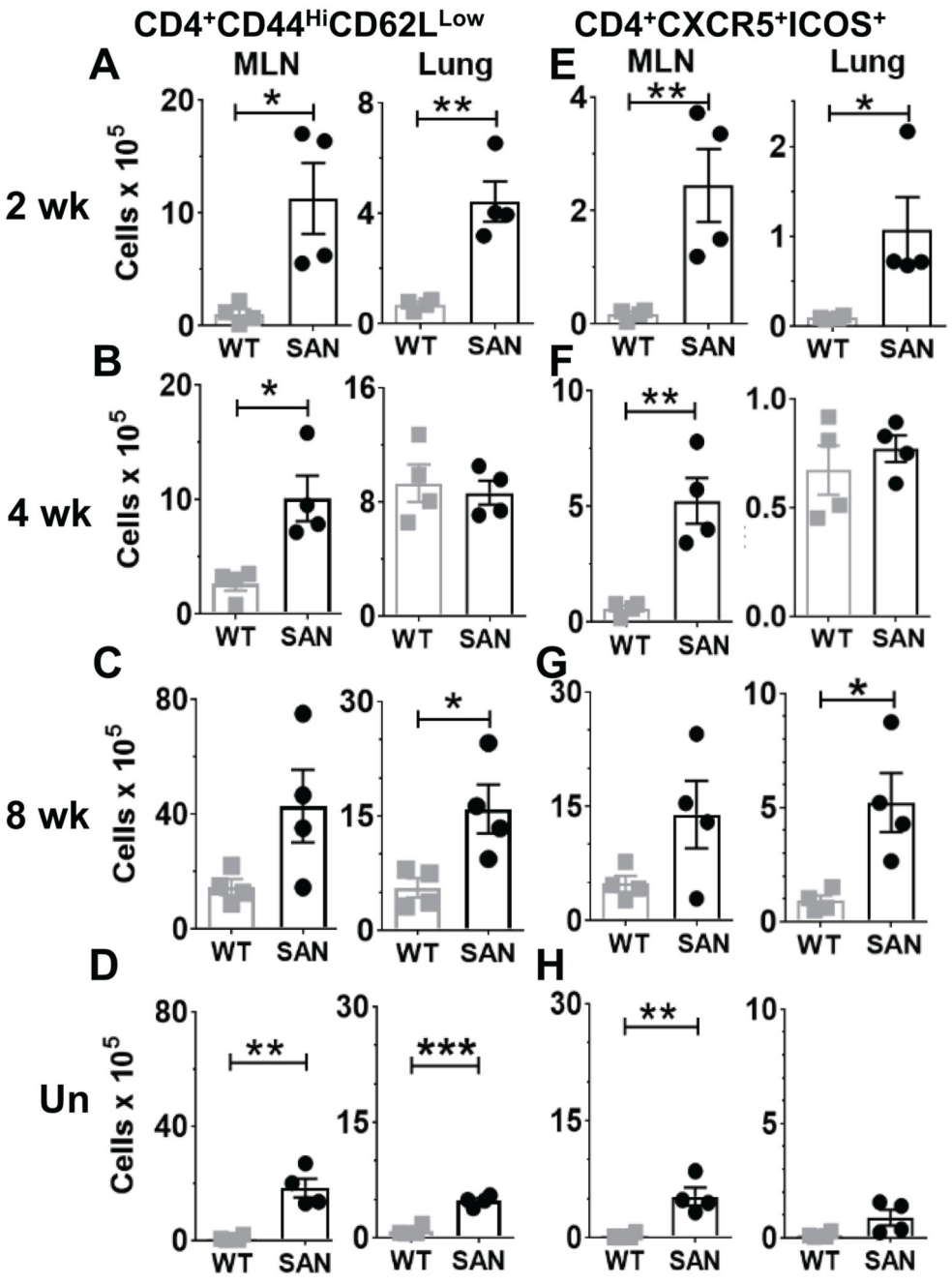

Figure 1. Increased numbers of activated T cells in *sanroque* mice during chronic *M. tuberculosis* infection.

WT ( ) and *sanroque* (SAN (●)) mice were infected with 100 CFU of *M. tuberculosis* by aerosol. At 2, 4, and 8 weeks post-infection T cell activation was analysed in the MLN and lung. *Sanroque* mice show increased numbers of activated $CD4^+$ ($CD44^{Hi}$ $CD62L^{Low}$) T cells in the MLN (A-C) at all times points examined regardless of infection. However, the numbers of activated $CD4^+$ T cells were enhanced in the lung of *sanroque* mice in response to infection at 8 weeks (C). Similarly, by 8 weeks the numbers of T_{FH}

Europe PMC Funders Author Manuscripts

($CD4^+CXCR5^+ICOS^+$) T cells were increased in the lung of *sanroque* mice due to infection (E-G). The numbers of activated T cells present in the MLN and lungs of uninfected mice harvested at the completion of the time course (14-16 weeks old) are represented in panel D and H. Data are the means ± SEM of 4 mice per group per time point and are representative of one of two independent experiments. The statistical differences between the mice were analysed by Student's *t* test, *P<0.05, **P<0.01 and ***P<0.001.

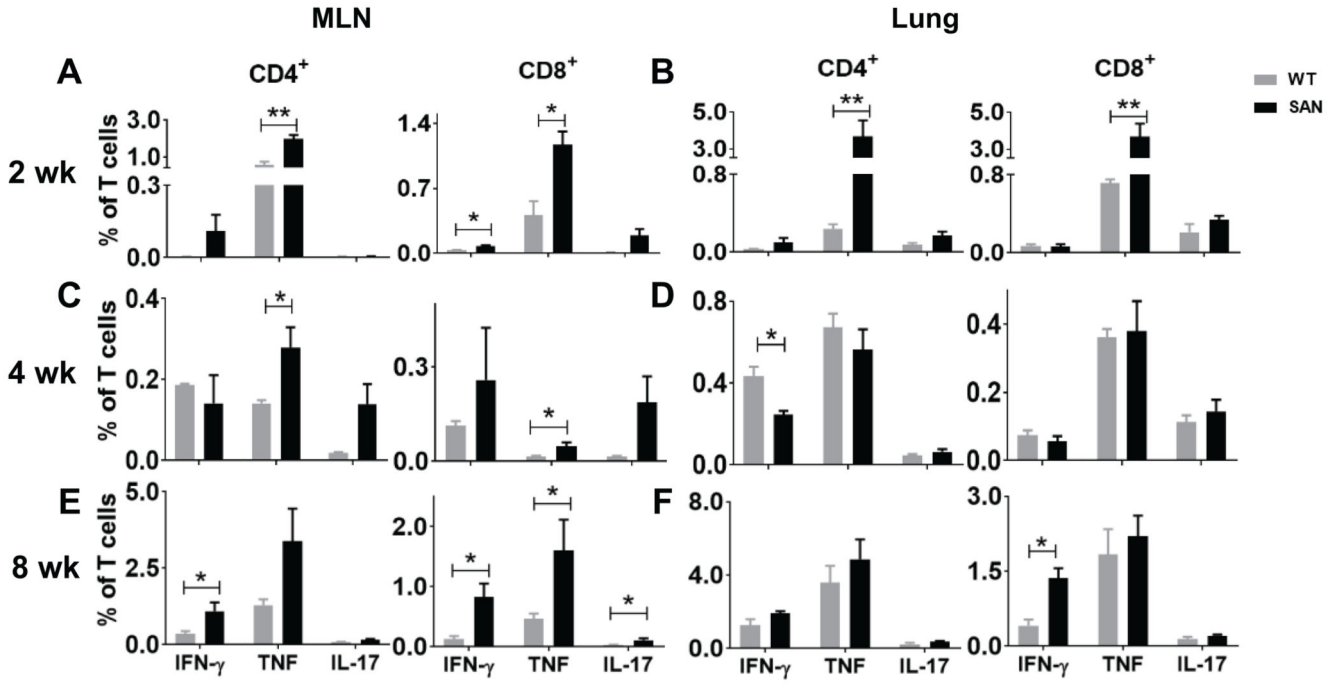

Figure 2. Enhanced antigen-specific cytokine production in *sanroque* mice during *M. tuberculosis* infection.

WT (grey) and *sanroque* (SAN) (black) mice (n=3-4) were infected with *M. tuberculosis* as described in Figure 1. At 2, 4 and 8 weeks post-infection antigen-specific cytokine production was analysed. *Sanroque* mice had higher percentages of antigen-specific TNF^+ IFN-γ^- $CD4^+$ and $CD8^+$ T cells but similar percentages of IFN-γ producing T cells in both the MLN (A) and lung (B), compared to WT mice following overnight stimulation with CFP at 2 weeks. At 4 weeks post-infection, the percentage of TNF^+ T cells were increased in the MLN (C) of *sanroque* mice but not in the lung (D). At 8 weeks, *sanroque* mice displayed increased percentages of IFN-γ positive $CD4^+$ and $CD8^+$ T cells in the MLN (E) and IFN-γ^+ $CD8^+$ T lung (F), with increased percentage of TNF positive T cells in the MLN but not in the lung. Data are the means ± SEM of 3-4 infected mice per group per time point and are representative of one of two independent experiments. The statistical differences between the mice were analysed by Student's *t* test, *P<0.05 and **P<0.01.

Europe PMC Funders Author Manuscripts

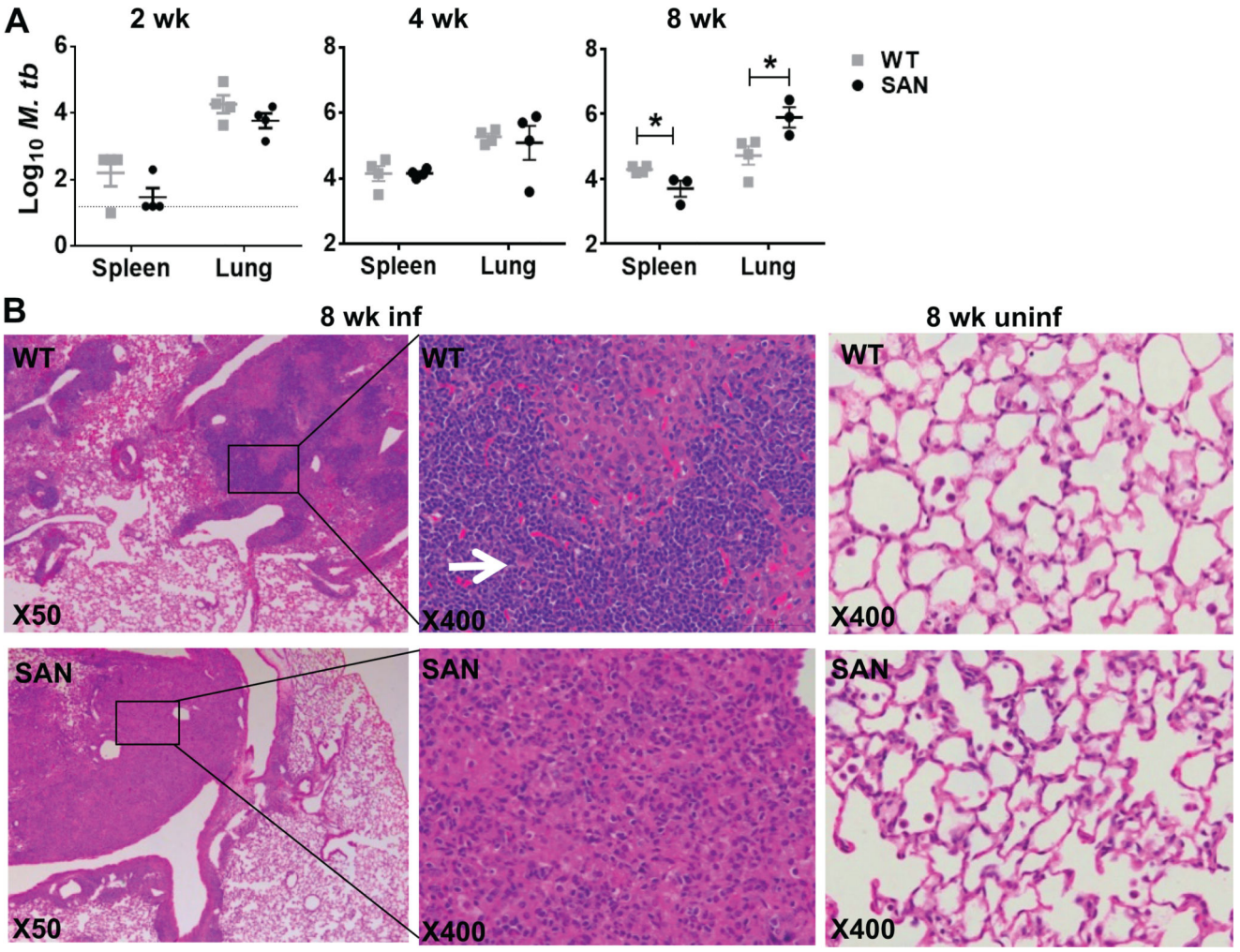

Figure 3. *Sanroque* mice showed increased bacterial burden in the lung associated with dysregulated inflammation and lack of lymphocytic aggregation during chronic *M. tuberculosis* infection.

WT and *sanroque* (SAN) mice (n=3-4) were infected with *M. tuberculosis* as described in Figure 1 and were euthanised 2, 4 and 8 weeks post-infection and *M. tuberculosis* load (Log_{10} CFU) in the spleen and lung determined. Compared to WT mice, *sanroque* mice showed a trend of delayed dissemination into the spleens (A). No difference in bacterial growth was seen at 4 weeks between the two groups of mice. However, *sanroque* mice had significantly increased bacterial burden in the lung compared to WT mice at 8 weeks post-infection. Analysis of H&E stained lung sections showed dysregulated inflammation in the *sanroque* mice compared to WT mice (B). In the WT mice section x400 magnification shows the lymphocyte cuff encompassing macrophages and monocytes (white arrow) whereas in the *sanroque* mice no such specific formations are evident with lymphocytes interwoven with macrophages and neutrophils in the lung. The lungs of uninfected mice show normal alveolar structure (B). The horizontal line in panel A is the limit of detection of bacteria. The data are the means ± SEM of 3-4 infected mice per group per time point and

are representative of one of three independent experiments. The significant differences between the infected groups of mice were analysed by Student's *t* test (* P<0.01).

Europe PMC Funders Author Manuscripts

Europe PMC Funders Author Manuscripts

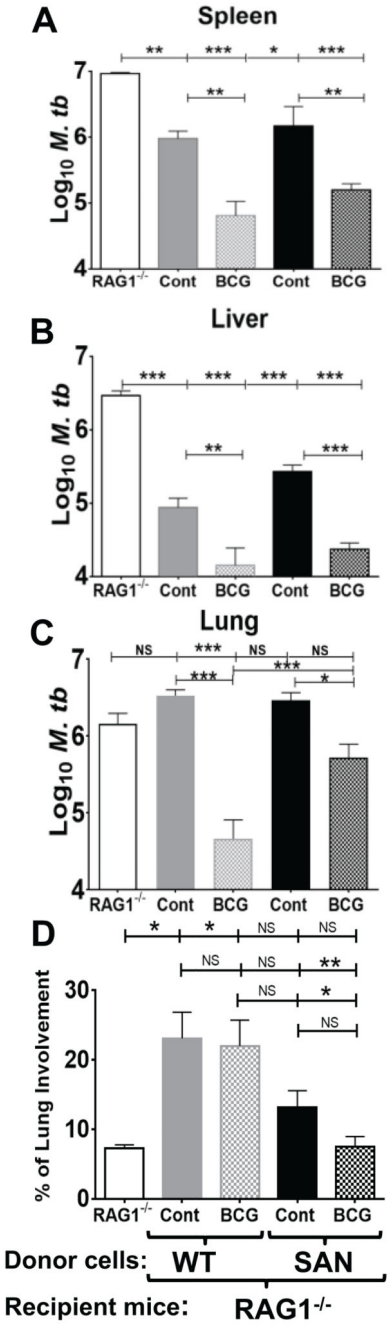

Figure 4. *M. bovis* BCG-primed *sanroque* T cells confer protection against *M. tuberculosis* infection.

WT and *sanroque* (SAN) mice were subcutaneously immunised with BCG, 3 weeks later cells from the draining lymph nodes of either immunized (BCG) or unimmunized (Cont) mice were harvested and cultured *in vitro* with BCG sonicate and mouse rIL-2 for 8 days. Expanded donor cells were transferred I.V. into recipient *Rag1*$^{-/-}$ (RAG1$^{-/-}$) mice, subsequently infected with *M. tuberculosis*. Both mycobacteria-specific WT and *sanroque* T cells enhanced protection against *M. tuberculosis* growth in the spleen (A), liver (B) and lung (C) at 18 days post-infection when compared with RAG1$^{-/-}$ mice receiving T cells from

unimmunised mice. The percentage of lung involvement was examined (D). Data are the means ± SEM of 5 mice per group and are representative of one of two independent experiments. The statistical differences were analysed by ANOVA *P<0.05, **P<0.01, ***P<0.001 and NS not significant

Europe PMC Funders Author Manuscripts

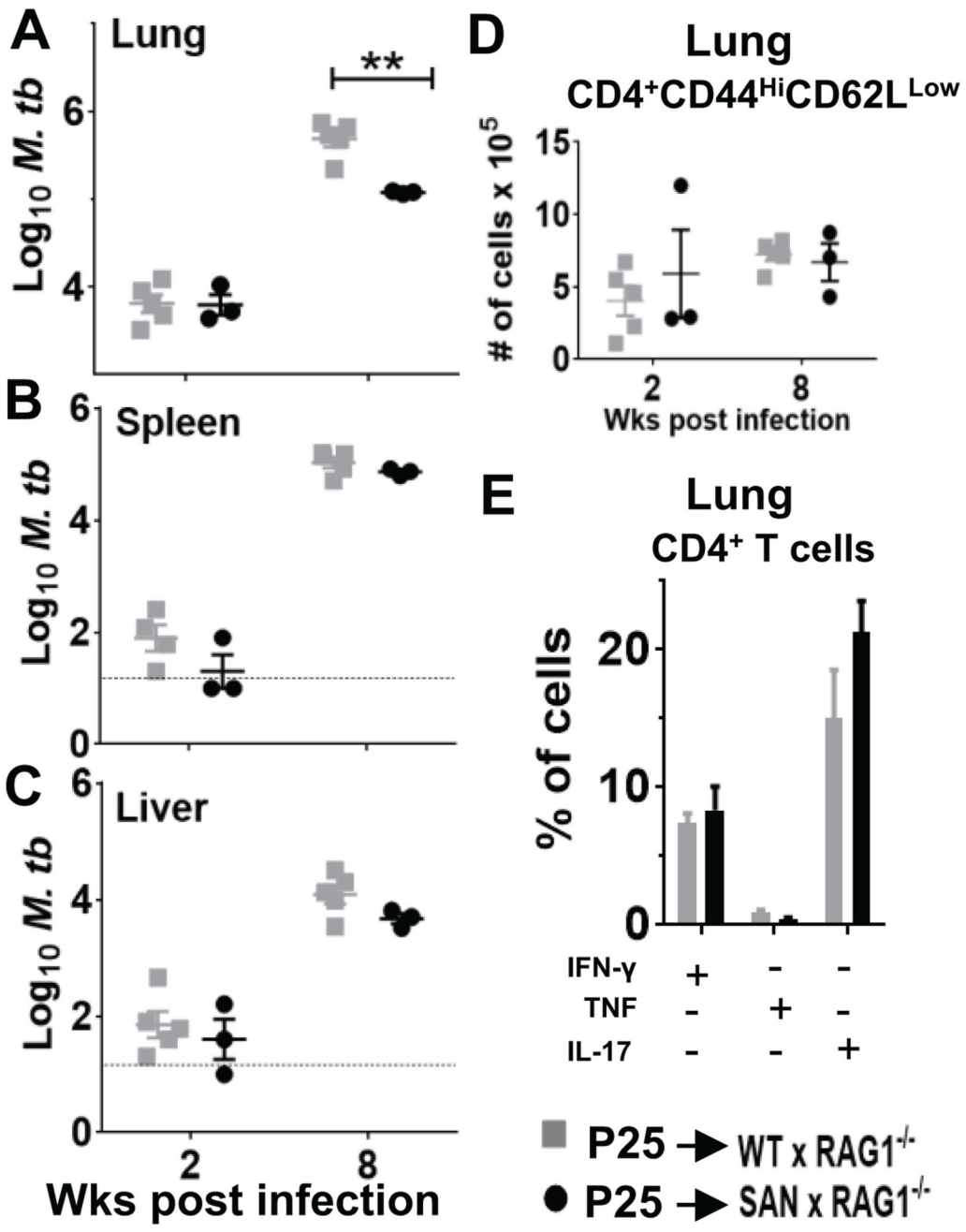

Figure 5. Enhanced control of chronic *M. tuberculosis* in *sanroque.Rag1*$^{-/-}$ mice recipients of mycobacterial-specific T cells.

Unprimed *M. tuberculosis*-specific splenocytes (from P25 Tg mice) were transferred into either WT.*Rag1*$^{-/-}$ (WT x RAG1$^{-/-}$ (/grey)) or *sanroque.Rag1*$^{-/-}$ (SAN x RAG1$^{-/-}$ (●/ black)) mice, infected 24 hours later with *M. tuberculosis* H37Rv by aerosol. Interestingly, *sanroque.Rag1*$^{-/-}$ mice showed significantly lower bacterial growth in the lung (A) compared to WT.*Rag1*$^{-/-}$ mice, though not in the spleen (B) and liver (C) at 8 weeks post-infection. The number of activated CD4^{+}CD44^{Hi}CD62L^{Low} T cells was similar in the lungs of WT.*Rag1*$^{-/-}$

and *sanroque.Rag1*$^{-/-}$ mice (D). T cells transferred into both groups of *Rag1*$^{-/-}$ mice displayed high percentages of IL-17 producing T cells in the lungs at 8 weeks post-infection (E). The horizontal lines are the limit of detection of bacteria Data are the means ± SEM of 3-4 infected mice per group per time point are representative of one of two independent experiments. The statistical differences between the mice were analysed by Student's *t* test, *P<0.05 and **P<0.01.

Europe PMC Funders Author Manuscripts

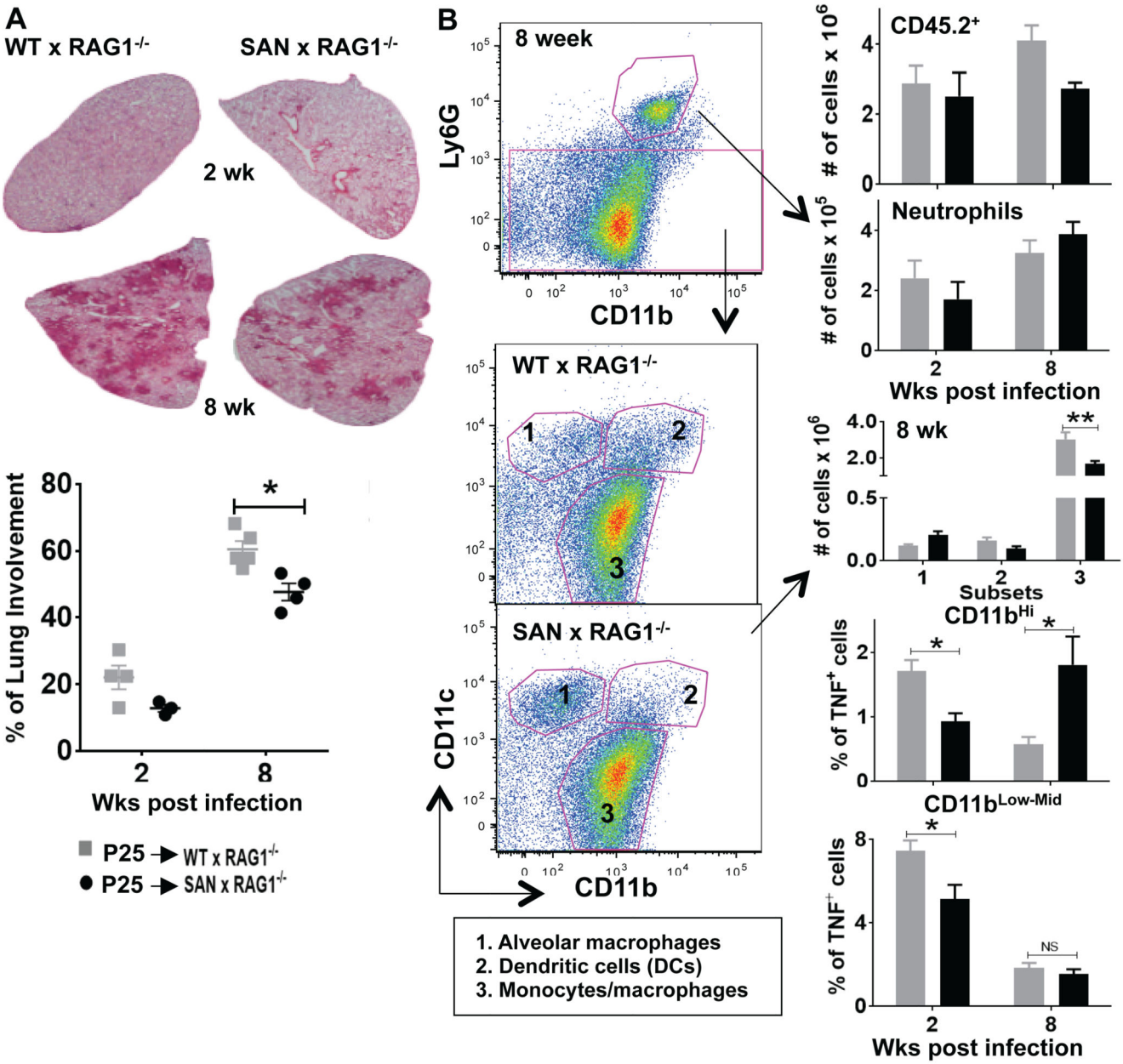

Figure 6. *Sanroque.Rag1*$^{-/-}$ mice show a reduced inflammatory response to *M. tuberculosis* infection.

WT.*Rag1*$^{-/-}$ (WT x RAG1$^{-/-}$(■)) or *sanroque.Rag1*$^{-/-}$ (SAN x RAG1$^{-/-}$ (●)) mice were infected with *M. tuberculosis* as described in Figure 5. The lower bacterial burden in the lungs of *sanroque.Rag1*$^{-/-}$ mice at 8 weeks post-infection (Fig 5A) was associated with significantly reduced lung inflammation (image ×12 magnification) (A). The CD45.2^{+} *Rag1*$^{-/-}$ cells were gated for neutrophils (CD11b^{Hi}Ly6G^{Hi}), then the remaining cells were characterised into alveolar macrophages (CD11b$^{Low\text{-}Mid}$CD11c^{Hi}/subset 1), dendritic cells (CD11b^{Hi}CD11c^{Hi}/subset 2) and monocytes/macrophages (CD11b$^{Mid\text{-}Hi}$CD11c$^{Low\text{-}Mid}$/ subset 3) (B). At 8 weeks, reduced numbers of monocytes/macrophages were evident in the

lungs of *sanroque.Rag1*$^{-/-}$ mice. Differences in the percentage of TNF producing myeloid cells (examined following overnight stimulation with CFP) were also seen (B). Data are the means ± SEM of 3-4 infected mice per group per time point and representative of one of two independent experiments. The statistical differences between the mice were analysed by ANOVA (*P<0.05, **P<0.01 and NS not significant).

Europe PMC Funders Author Manuscripts

Europe PMC Funders Author Manuscripts

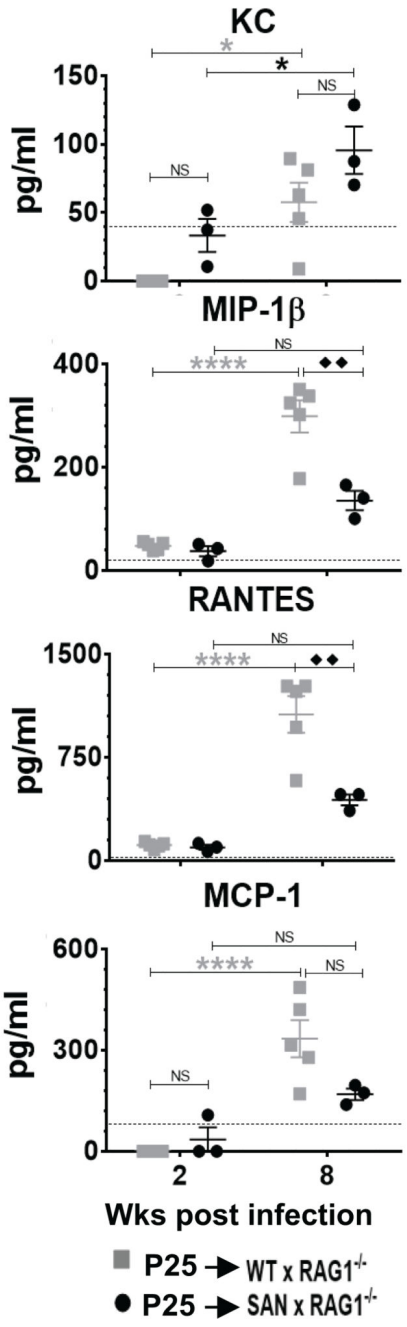

Figure 7. Reduced levels of MIP-1β and RANTES in *sanroque.Rag1*$^{-/-}$ mice following *M. tuberculosis* infection.

WT.*Rag1*$^{-/-}$ (WT x RAG1$^{-/-}$ ( )) or *sanroque.Rag1*$^{-/-}$ (SAN x RAG1$^{-/-}$ (●)) mice were infected with *M. tuberculosis* as described in Figure 5. Chemokines released in the lung homogenates were examined by CBA. The transfer of mycobacterial-specific T cells into the *sanroque.Rag1*$^{-/-}$ mice was associated with reduced production of MIP-1β, RANTES and MCP-1 at 8 weeks post-infection. The horizontal lines are limit of detection for each chemokine. Data are the mean ± SEM of 3-5 infected mice per group per time point and are

representative of one of two independent experiments. The significant differences were analysed by ANOVA, *P<0.05, ♦♦ or **P<0.01, ****P<0.0001 and NS not significant.

Europe PMC Funders Author Manuscripts